BRAIN
ORIGINAL ARTICLE

# Predicting amyloid PET and tau PET stages with plasma biomarkers

Clifford R. Jack Jr,[1] Heather J. Wiste,[2] Alicia Algeciras-Schimnich,[3] Dan J. Figdore,[3] Christopher G. Schwarz,[1] Val J. Lowe,[4] Vijay K. Ramanan,[5] Prashanthi Vemuri,[1] Michelle M. Mielke,[6] David S. Knopman,[5] Jonathan Graff-Radford,[5] Bradley F. Boeve,[5] Kejal Kantarci,[1] Petrice M. Cogswell,[1] Matthew L. Senjem,[1] Jeffrey L. Gunter,[1] Terry M. Therneau[2] and Ronald C. Petersen[5]

**See Mattsson-Carlgren and Palmqvist (https://doi.org/10.1093/brain/awad112) for a scientific commentary on this article.**

Staging the severity of Alzheimer's disease pathology using biomarkers is useful for therapeutic trials and clinical prognosis. Disease staging with amyloid and tau PET has face validity; however, this would be more practical with plasma biomarkers. Our objectives were, first, to examine approaches for staging amyloid and tau PET and, second, to examine prediction of amyloid and tau PET stages using plasma biomarkers.

Participants ($n = 1136$) were enrolled in either the Mayo Clinic Study of Aging or the Alzheimer's Disease Research Center; had a concurrent amyloid PET, tau PET and blood draw; and met clinical criteria for cognitively unimpaired ($n = 864$), mild cognitive impairment ($n = 148$) or Alzheimer's clinical syndrome with dementia ($n = 124$). The latter two groups were combined into a cognitively impaired group ($n = 272$). We used multinomial regression models to estimate discrimination [concordance (C) statistics] among three amyloid PET stages (low, intermediate, high), four tau PET stages (Braak 0, 1–2, 3–4, 5–6) and a combined amyloid and tau PET stage (none/low versus intermediate/high severity) using plasma biomarkers as predictors separately within unimpaired and impaired individuals. Plasma analytes, p-tau181, $A\beta_{1–42}$ and $A\beta_{1–40}$ (analysed as the $A\beta_{42}/A\beta_{40}$ ratio), glial fibrillary acidic protein and neurofilament light chain were measured on the HD-X Simoa Quanterix platform. Plasma p-tau217 was also measured in a subset ($n = 355$) of cognitively unimpaired participants using the Lilly Meso Scale Discovery assay.

Models with all Quanterix plasma analytes along with risk factors (age, sex and APOE) most often provided the best discrimination among amyloid PET stages (C = 0.78–0.82). Models with p-tau181 provided similar discrimination of tau PET stages to models with all four plasma analytes (C = 0.72–0.85 versus C = 0.73–0.86). Discriminating a PET proxy of intermediate/high from none/low Alzheimer's disease neuropathological change with all four Quanterix plasma analytes was excellent but not better than p-tau181 only (C = 0.88 versus 0.87 for unimpaired and C = 0.91 versus 0.90 for impaired). Lilly p-tau217 outperformed the Quanterix p-tau181 assay for discriminating high versus intermediate amyloid (C = 0.85 versus 0.74) but did not improve over a model with all Quanterix plasma analytes and risk factors (C = 0.85 versus 0.83).

Plasma analytes along with risk factors can discriminate between amyloid and tau PET stages and between a PET surrogate for intermediate/high versus none/low neuropathological change with accuracy in the acceptable to excellent range. Combinations of plasma analytes are better than single analytes for many staging predictions with the exception that Quanterix p-tau181 alone usually performed equivalently to combinations of Quanterix analytes for tau PET discrimination.

Received September 09, 2022. Revised December 20, 2022. Accepted January 21, 2023. Advance access publication February 15, 2023

1 Department of Radiology, Mayo Clinic, Rochester, MN 55905, USA
2 Department of Quantitative Health Sciences, Mayo Clinic, Rochester, MN 55905, USA
3 Department of Laboratory Medicine, Mayo Clinic, Rochester, MN 55905, USA
4 Department of Nuclear Medicine, Mayo Clinic, Rochester, MN 55905, USA
5 Department of Neurology, Mayo Clinic, Rochester, MN 55905, USA
6 Department of Epidemiology and Prevention, Wake Forest University School of Medicine, Winston-Salem, NC 27101, USA

Correspondence to: Clifford R. Jack, Jr, MD
200 First St. SW, Rochester, MN 55905, USA
E-mail: jack.clifford@mayo.edu

Keywords: amyloid PET; tau PET; staging Alzheimer's disease; plasma biomarkers; Alzheimer's biomarkers

## Introduction

Development of plasma biomarkers has been the most important recent advancement in Alzheimer's disease diagnostics. Recent reports have shown the diagnostic and prognostic potential of several plasma analytes, including plasma $A\beta_{42}/A\beta_{40}$ (which correlates with CSF and amyloid PET, and predicts clinical progression),[1–7] plasma phosphorylated tau (p-tau) proteoforms[8–11] (which predict future clinical progression[12–15] and correlate with CSF,[8,9,11,16–19] PET[6,8,11,18,20–22] and post-mortem measures of Alzheimer's disease neuropathological change[10,11,16,21,23–25]), plasma neurofilament light chain (NfL, a marker of large-calibre axonal injury in various disorders that is associated with higher risk of incident dementia)[26–34] and plasma glial fibrillary acidic protein (GFAP, a marker of astrocytic activation that is associated with higher risk of incident dementia and faster rates of cognitive decline).[6,31,32,34–38]

Biomarkers are often classified in a binary manner—normal versus abnormal; furthermore, the cut-off point is often set at the detection threshold limit. However, staging the severity of biomarker abnormalities has important uses. For example, in the A4 and AHEAD studies, inclusion/exclusion or arm assignment within the trial is based on amyloid PET severity/stage, not normal/abnormal.[39,40] Inclusion in the Trailblazer-Alz study was based on tau PET stage and dosing modifications during the study were based on amyloid PET stage.[41] Staging the severity of Aβ and tau pathology is also relevant for clinical prognosis. The lifetime risk of developing dementia is significantly greater in individuals with higher amyloid PET stages.[42] Higher tau and amyloid PET burden is associated with greater rates of cognitive decline among unimpaired individuals.[43] Rates of tau PET accumulation are greater in unimpaired individuals with a high amyloid PET stage.[44,45]

Amyloid and tau severity can be staged by PET using either topographic distributions[46–60] or quantitative region of interest–based cut-off points.[61–63] In most settings, however, it would be far more practical to stage disease with plasma biomarkers as opposed to acquiring two separate PET scans. In addition to cost and accessibility, an obvious advantage of plasma biomarkers over PET imaging is the ability to measure several different analytes from a single venipuncture. An understudied question, however, is whether combinations of plasma analytes improve disease staging accuracy over a single highly efficient analyte. In addition, measures of multiple analytes would be far more efficient if all could be run on the same platform as opposed to needing different platforms potentially requiring different central labs.

Our first objective in this study was to examine approaches for staging amyloid PET and tau PET based on both topography (location) and magnitude (uptake in a prespecified meta-region of interest). From this, we selected optimal PET staging methods—magnitude for amyloid PET and both topographic and magnitude staging for tau PET—for analyses with plasma biomarkers. Here, we leveraged the Quanterix HD-X Simoa platform which is commercially available and measures $A\beta_{1–42}$ and $A\beta_{1–40}$, GFAP and NfL as a multiplex assay and p-tau181 as a singleplex assay. We then examined discrimination among amyloid and tau PET pathological stages using these Quanterix plasma biomarkers, first testing how well each analyte performed individually (when added to a base model consisting of established risk factors) and, second, testing if PET staging discrimination was improved when all plasma analytes were entered into a model simultaneously. Plasma p-tau217 was also measured in a subset of cognitively unimpaired (CU) participants using the Lilly Meso Scale Discovery (MSD) assay. Because most relevant applications of plasma-based pathological staging would have different implications for cognitively unimpaired versus impaired individuals, we examined discrimination of PET-defined stages separately for these two groups as well as among all participants combined.

## Material and methods

### Enrolment and clinical characterization

This study was approved by the Mayo Clinic and Olmsted Medical Center Institutional Review Boards. Written informed consent was obtained from all participants and in the case of persons with cognitive impairment sufficient to interfere with capacity, from a close family member.

All individuals in this study were enrolled in one of two studies. The Mayo Clinic Study of Aging (MCSA) is a longitudinal population-based study of cognitive ageing among a stratified random sample of residents of Olmsted County, Minnesota, USA.[64] The Mayo Alzheimer's Disease Research Center (ADRC) is a longitudinal research study of individuals recruited from clinical practice.

Participants in both studies were assigned a diagnosis of cognitively unimpaired [defined as not mild cognitive impairment (MCI) or dementia], MCI[65] or dementia[66] using established criteria. Individuals with dementia had received diagnoses consistent with Alzheimer's clinical syndrome (referred to as AlzCS dem),[67] which included the typical amnestic phenotype and established atypical Alzheimer's disease phenotypes.[68] MCI and AlzCS dem participants were combined into a cognitively impaired (CI) group.

For inclusion, a person must have been a participant in the MCSA or ADRC aged 50 years or older; had concurrent amyloid PET, tau PET, MRI (MR is used for PET quantification) and a blood draw; and have met the above criteria for membership in one of the three clinical diagnostic groups described.

## Imaging methods

Amyloid PET imaging was performed with Pittsburgh Compound B[69] and tau PET with flortaucipir.[70] MRI was performed at 3 T and was used in the PET data processing pipeline.[71] PET target and reference regions of interest were defined using the Mayo MCALT atlas with a previously described processing pipeline.[71] Amyloid and tau PET standardized uptake value ratios (SUVR) were formed by normalizing target regions of interest to the cerebellar crus grey matter.[61]

## Amyloid PET staging

Two methods of staging amyloid PET were implemented. To avoid confusion between them, we labelled topographic staging using a numbered stage and magnitude staging using categories of none/low, intermediate and high.

### Topographic staging

Amyloid PET regions were grouped into five stages based on recommendations by Collij *et al.*[48] and labelled as A0, A1, A2, A3, A4. Anatomic descriptions and images (Supplementary Fig. 1) of these stages are in the Supplementary material, which also includes more detailed methods of the topographic staging and cut-off points (Supplementary Fig. 2 and Supplementary material PET methods).

### Magnitude staging

The amyloid PET target cortical meta-region of interest included the prefrontal, orbitofrontal, parietal, temporal, precuneus and anterior and posterior cingulate cortices (Supplementary Fig. 1).[61] Two previously established cut-off points (SUVR = 1.48, centiloid = 22 and SUVR = 2.0, centiloid = 68)[44,72] were used to segment the continuous cortical meta-region of interest range into three groups: none/low, $A^{LOW}$; intermediate, $A^{INT}$; and high, $A^{HIGH}$.

## Tau PET staging

Two methods of staging tau PET were implemented. To avoid confusion, we labelled tau PET topographic staging using standard Braak stage terminology and tau PET magnitude staging using categories of none/low, intermediate and high.

### Topographic staging

We defined four topographic stages based on Braak-like[73] PET staging schemes described by others[51–60]: Braak stage 0, 1–2, 3–4, 5–6. Anatomic descriptions and images (Supplementary Fig. 1) of these stages are in the Supplementary material, which also includes more detailed methods of the topographic staging and cut-off points (Supplementary Fig. 2 and Supplementary material PET methods).

### Magnitude staging

A tau PET temporal lobe target meta-region of interest used in prior analyses was formed that included the amygdala, entorhinal cortex, fusiform, parahippocampal, inferior temporal gyrus and middle temporal gyrus (Supplementary Fig. 1).[61] Two cut-off points were selected, SUVR = 1.29 and SUVR = 1.43, to segment the continuous SUVR range in the temporal meta-region of interest into three groups: none/low, $T^{LOW}$; intermediate, $T^{INT}$; and high, $T^{HIGH}$. The lower cut-off point of 1.29 was previously established by a neuropathological standard,[74] while the upper cut-off point of 1.43 was determined in this study from the lower quartile of the meta-region of interest SUVR in the Braak 3–4 group (Fig. 1).

## Combined amyloid and tau PET staging

A combination of the amyloid magnitude stage and the tau PET topographic stage was used as a proxy of Alzheimer's disease neuropathological change. Participants with the conjunction of $A^{INT}$ or $A^{HIGH}$ and Braak 3–4 or 5–6 were categorized as intermediate to high severity of Alzheimer's disease neuropathological change, while participants with $A^{LOW}$ or Braak 0 or 1–2 were categorized as none/low severity of Alzheimer's disease neuropathological change.

## Plasma analyte measures

EDTA-plasma samples were collected from participants after an overnight fast. Samples were centrifuged, and 500 µl of plasma was aliquoted into polypropylene tubes and stored at −80°C until testing. Plasma $A\beta_{1-40}$, $A\beta_{1-42}$, GFAP and NfL were measured using the Simoa Neurology 4-Plex E Advantage kit (N4PE, item #103670). Plasma phospho-Tau 181 (pTau-181) was measured with the Simoa pTau-181 Advantage V2 kit (item #103714). Both kits were used per manufacturer's instructions and run on a Quanterix HD-X analyser (Quanterix). Briefly, after thawing and mixing, plasma samples were centrifuged for 5 min × 4000*g*. Samples were diluted 1:4 using the instrument's on-board dilution protocol and tested in singlet. A seven-point calibration curve and sample concentrations were determined on the Simoa HD-X analyser software using a weighting factor of $1/y^2$ and a 4-parameter logistic curve fitting algorithm for p-tau181. The N4PE test used eight-point calibration curves with $1/y^2$ weighting; a four-parameter logistic fitting algorithm was used for NfL and GFAP, while a five-parameter logistic fitting algorithm was used for $A\beta_{1-40}$ and $A\beta_{1-42}$. Two levels of quality control material were run in duplicate with each batch following the assay calibrators. Inter-assay imprecision for the quality control material (expressed as % coefficient of variation) were as follows: $A\beta_{1-40}$, 5% and 3% at approximate concentrations of 16 and 117 pg/ml; $A\beta_{1-42}$, 4% and 7% at approximate concentrations of 5.5 and 31 pg/ml; GFAP, 7% and 7% at approximate concentrations of 181 and 3702 pg/ml; NfL, 12% and 14% at approximate concentrations of 21 and 432 pg/ml; p-tau181, 6% and 5% at approximate concentrations of 3.7 and 119 pg/ml. The ratio of $A\beta_{1-42}$ to $A\beta_{1-40}$ was created and used in the statistical analysis.

Plasma p-tau217 was also measured in a subset of CU participants on the MSD platform by electrochemiluminescence using proprietary assays developed by Lilly Research Laboratories.[22] Samples were diluted 1:2, and 50 µl of diluted sample was used for each replicate. The assay was performed on a small spot streptavidin plate using biotinylated IBA493 (anti-phosphorylated Thr217 tau monoclonal antibody developed by Lilly Research Laboratories, 0.5 µg/ml) as the capture. SULFO-4G10-E2 (anti-tau monoclonal antibody developed by Lilly Research Laboratories, 0.02 µg/ml) was the detector. The assay was calibrated using a synthetic p-tau peptide coupled with a polyethylene glycol linker to a second tau peptide matching amino acids 111–130 according to the Tau441 sequence numbering.

## Statistical methods

Differences in participant characteristics across the clinical diagnosis groups were tested with Kruskal–Wallis or pairwise Wilcoxon rank-sum tests for continuous variables and chi-squared tests for categorical variables.

The analytic approach was designed to address two overall questions. First, if adding each analyte individually to a base model

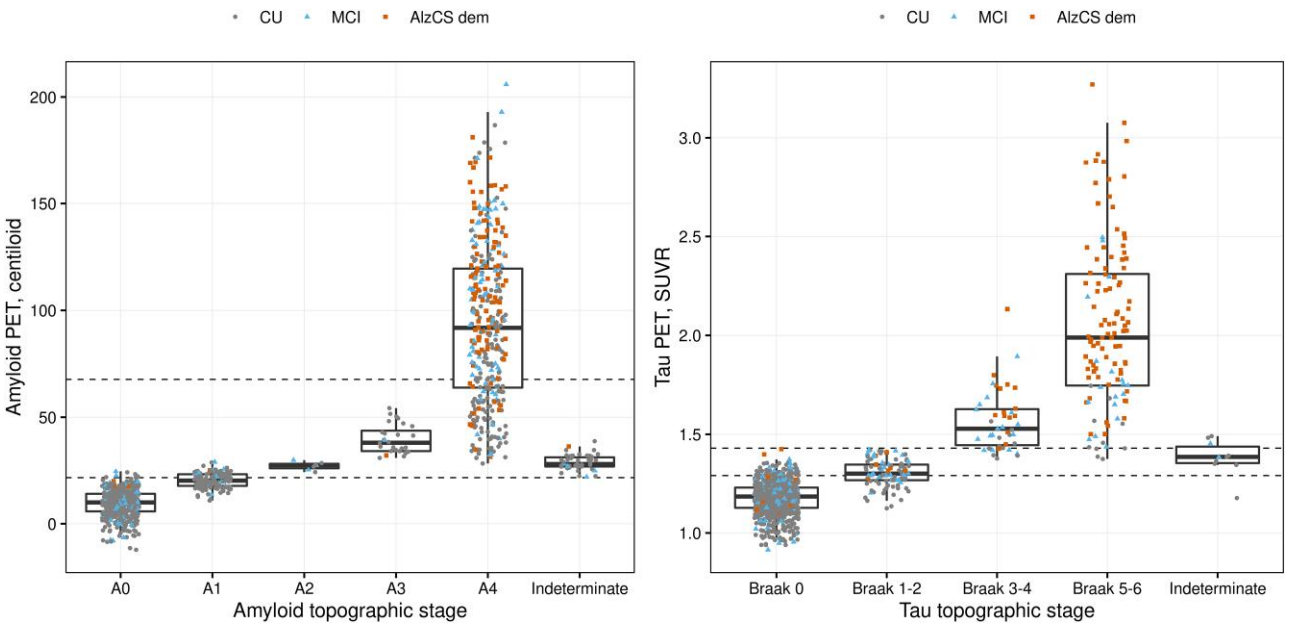


**Figure 1 Topographic staging of amyloid and tau PET**. Box plots of meta-region of interest PET values by PET topographic stage for amyloid PET and tau PET.

of risk factors improved staging discrimination over the base model, and second, testing if PET staging discrimination was improved when all plasma analytes were entered into a model simultaneously. Multinomial regression models were used to estimate the associations between the continuous plasma biomarker predictors and the categorical amyloid and tau PET stage outcomes. (We chose to use multinomial regression models because, even though the stages are ordered, we did not want to make the strong assumptions inherent in ordinal logistic models about the relationship between plasma biomarkers and relative odds of the different PET stages.) For a binary outcome, a multinomial model simplifies to a logistic model. Models were fit separately for each outcome (amyloid PET magnitude stage, tau PET topographic stage, tau PET magnitude stage and a combined amyloid and tau PET stage used as a proxy for Alzheimer's disease neuropathological change) and separately within CU and CI participants. For the primary analysis, a series of models with different predictors were fit for each outcome and participant group. First, a 'base' model was fit with risk factors of age, sex and APOE $\epsilon$4 genotype as predictors. Next, each plasma biomarker was added separately to this base model. Lastly, a full model was fit with age, sex, APOE and all four Quanterix plasma biomarkers ($A\beta_{42}/A\beta_{40}$, p-tau181, NfL and GFAP). In a secondary analysis, models were fit with the plasma biomarkers (individually or combined) without adjusting for the base model.

Additionally, models were fit with CU and CI participants combined and the base risk factor model included age, sex, APOE a three-level study/diagnosis variable (MCSA-CU, MCSA-CI, ADRC-CI) and an interaction with age and study/diagnosis.

P-tau181, GFAP and NfL measurements were log-transformed due to skewness in the data distributions. For tau PET staging, as few CU participants were in Braak stages 3–4 and 5–6, we combined these two tau PET subsets in the CU group analyses. Odds ratios were summarized for each model as a measure of the association between the predictor variables and PET stage outcomes. Additionally, we used the linear predictor from each model to estimate concordance (C) statistics for the comparisons of PET stage pairs. The C statistic serves as an overall measure of discrimination and is equivalent to the area under the curve (AUC) for binary outcomes (here pairs of PET stages). C statistic values between 0.7 and 0.8 represent 'acceptable', 0.8–0.9 'excellent' and above 0.9 'outstanding' discrimination.[75] A jackknife approach was used to test for differences in C statistics across models having different predictor variables but the same PET stage outcome and the same participants. Confidence intervals for C statistics and differences in C statistics were calculated using the log[p/(1–p)] (i.e. logit) transformation, commonly used for binomial data.

Additionally, in a subset of CU participants with Quanterix measures and Lilly p-tau217, models were fit with and without base risk factors to compare the p-tau assays and to compare the Lilly p-tau217 models to models with all four Quanterix measures. Due to small numbers of participants in this subset with high tau values, tau PET stages were grouped as Braak 1–6 versus Braak 0 and $T^{HIGH/INT}$ versus $T^{LOW}$.

All analyses were done using the R language and environment for statistical computing version 4.1.2.

## Data availability

Data from the Mayo Clinic Study of Aging and the Alzheimer's Disease Research Center are available to qualified academic and industry researchers by request to the MCSA and ADRC Executive Committee (https://www.mayo.edu/research/centers-programs/alzheimers-disease-research-center/research-activities/mayo-clinic-study-aging/for-researchers/data-sharing-resources).

# Results

## Study participants

A total of 1136 participants met the inclusion criteria: 864 CU, 148 MCI and 124 AlzCS dem (Table 1). Amyloid PET centiloid and tau PET temporal meta-region of interest SUVR values were greatest in the AlzCS dem group and least in the CU group ($P < 0.001$ for all). Plasma $A\beta_{42}/A\beta_{40}$ was lower in the AlzCS dem group compared

to the CU and MCI groups ($P < 0.001$ for both), but were more similar between the CU and MCI groups ($P = 0.10$; Table 1). Plasma p-tau181, GFAP and NfL all differed by group ($P \leq 0.01$ for all) and were lowest in the CU and highest in the AlzCS dem group. Clinical and biomarker characteristics of the Lilly CU subset, $n = 355$, were very similar to those of the larger CU study cohort.

## Amyloid PET staging

### Topographic staging

Seventy-one percent of CU participants were in stages A0 or A1 ($n$ = 616), while 70% of CI participants were in A4 ($n = 191$). Very few participants (CU or CI) were in the A2 ($n = 7$) and A3 ($n = 28$) stages (Fig. 1 and Supplementary Table 1) and 46 (4%) individuals did not fit this staging scheme and therefore were classified as indeterminate. SUVR values in the regional amyloid PET regions of interest used to define the topographic staging were all highly correlated ($r$ values ranged from 0.96 to 0.98), indicating that successive topographic stages of amyloid PET did not capture unique information versus SUVR-based burden across these regions of interest (Supplementary Fig. 3).

### Magnitude staging

Sixty-five percent of CU were in $A^{LOW}$ while 60% of CI were in $A^{HIGH}$ (Table 1). The lower magnitude cut-off point (centiloid 22) fell near the median of the meta-region of interest centiloid in the A1 stage and the upper cut-off point (centiloid 68) fell just above the lower quartile of the meta-region of interest centiloid in the A4 stage, suggesting good performance of these cut-off points for discrimination of degrees of amyloid PET burden (Fig. 1). For all the above reasons, we elected to use only magnitude staging of amyloid PET for the analyses with plasma biomarkers.

## Tau PET staging

### Topographic staging

Ninety percent of CU participants were in Braak stage 0 while 71% of AlzCS dem participants were in Braak stage 5–6 (Table 1). Topographic staging resulted in only 10 (under 1%) individuals staged as indeterminate. Correlations in SUVR values among the regional tau PET regions of interest used to define topographic staging were high for Braak 3–4 and 5–6 ($r = 0.94$) but lower compared to correlations with Braak 1–2 ($r = 0.85$ and 0.76), indicating that this topographic staging approach captures unique information (Supplementary Fig. 4).

### Magnitude staging

The lower magnitude tau PET cut-off point (SUVR = 1.29) fell near the median of the meta-region of interest SUVR in the Braak 1–2 group. The upper cut-off point (SUVR 1.43) was defined by the lower quartile of the meta-region of interest SUVR in the Braak 3–4 group (Fig. 1 and Supplementary Table 2).

## Distribution of plasma biomarker findings by amyloid and tau PET stage

Median $A\beta_{42}/A\beta_{40}$ decreased and p-tau181, GFAP and NfL increased with increasing amyloid PET stages (Fig. 2). The most pronounced difference between tau PET stages for all four plasma analytes was between Braak 0 and Braak 1–2. There was considerable overlap in plasma values among individual participants across amyloid and tau PET stages with all four plasma analytes.

## Predicting amyloid PET stages with Quanterix plasma biomarkers

Our primary results are reported as C statistics for the different models using Quanterix plasma biomarkers to discriminate amyloid PET and tau PET stages (Figs 3–5). The C statistic is equivalent to the AUC for discriminating pairs of PET stages, and therefore the ROC curves that correspond to the C statistics are also shown. Detailed odds ratios from all models are found in Supplementary Tables 3–5.

Among CU participants (Fig. 3) for amyloid PET, $A\beta_{42}/A\beta_{40}$ (C = 0.77) and p-tau181 (C = 0.76) each improved discrimination of $A^{INT}$ versus $A^{LOW}$ when individually added to the base model of age, sex and APOE (C = 0.74; $P = 0.001$ and $P = 0.03$, respectively). $A\beta_{42}/A\beta_{40}$ (C = 0.71), p-tau181 (C = 0.72) and GFAP (C = 0.72) improved discrimination of $A^{HIGH}$ versus $A^{INT}$ when individually added to the base model (C = 0.67; $P = 0.03$, $P = 0.01$, $P = 0.04$, respectively). The models with all four plasma analytes plus base improved discrimination over the base model and any of the models with individual analytes for both $A^{INT}$ versus $A^{LOW}$ (C = 0.80, $P < 0.05$ for all) and $A^{HIGH}$ versus $A^{INT}$ (C = 0.78, $P \leq 0.01$ for all).

Among CI participants for amyloid PET (Fig. 4), the model with all four plasma analytes improved discrimination of $A^{INT}$ versus $A^{LOW}$ when added to the base model (C = 0.72 versus 0.61, $P = 0.04$). For $A^{HIGH}$ versus $A^{INT}$, the model with p-tau181 improved discrimination when added to the base model (C = 0.78 versus 0.70, $P = 0.02$). The model with all four plasma analytes plus base (C = 0.82, $P \leq 0.03$) improved discrimination of $A^{HIGH}$ versus $A^{INT}$ over any of the models with individual analytes and over the base model.

When CU and CI participants were combined (Fig. 5), $A\beta_{42}/A\beta_{40}$ (C = 0.77) and p-tau181 (C = 0.77) each improved discrimination of $A^{INT}$ versus $A^{LOW}$ when individually added to the base model of age, sex, APOE, a three-level study/clinical diagnosis variable and an interaction with age and study/diagnosis (C = 0.75; $P = 0.002$ and $P = 0.02$, respectively). $A\beta_{42}/A\beta_{40}$ (C = 0.81), p-tau181 (C = 0.83) and GFAP (C = 0.82) improved discrimination of $A^{HIGH}$ versus $A^{INT}$ when individually added to the base model (C = 0.80; $P = 0.048$, $P = 0.002$, $P = 0.03$, respectively). The model with all four plasma analytes plus base improved discrimination over the base model and any of the models with individual analytes for both $A^{INT}$ versus $A^{LOW}$ (C = 0.79, $P \leq 0.02$) and $A^{HIGH}$ versus $A^{INT}$ (C = 0.85, $P \leq 0.04$ for all).

## Predicting tau PET stages with Quanterix plasma biomarkers

Among CU participants for tau PET (Fig. 3), p-tau181 improved discrimination of Braak 1–2 versus Braak 0 (C = 0.81 versus 0.77, $P = 0.02$) and $T^{INT}$ versus $T^{LOW}$ (C = 0.72 versus 0.69, $P = 0.02$) when added to the base model. For Braak 1–2 versus Braak 0 (C = 0.83) and $T^{INT}$ versus $T^{LOW}$ (C = 0.73) the models with all four plasma analytes improved discrimination over any of the models with individual analytes ($P \leq 0.01$ for all) except the model with p-tau181. For Braak 3–6 versus Braak 1–2 (C = 0.67–0.68 versus 0.67) and $T^{HIGH}$ versus $T^{INT}$ (C = 0.79–0.84 versus 0.79), none of the plasma analytes alone or in combination significantly improved on the base model.

**Table 1 Characteristics of participants**

| | All | | | Lilly subset |
|---|---|---|---|---|
| | CU ($n = 864$) | MCI ($n = 148$) | AlzCS dem ($n = 124$) | CU ($n = 355$) |
| Study | | | | |
| ADRC | 0 (0%) | 52 (35%) | 117 (94%) | 0 (0%) |
| MCSA | 864 (100%) | 96 (65%) | 7 (6%) | 355 (100%) |
| Age, years | | | | |
| Median (Q1, Q3) | 70 (64, 79) | 75 (69, 82) | 70 (62, 78) | 71 (65, 80) |
| Range | 50–98 | 52–98 | 52–89 | 52–98 |
| Sex | | | | |
| Female | 413 (48%) | 60 (41%) | 70 (56%) | 170 (48%) |
| Male | 451 (52%) | 88 (59%) | 54 (44%) | 185 (52%) |
| APOE $\epsilon$4 genotype | | | | |
| Non-carrier | 611 (71%) | 83 (56%) | 38 (31%) | 247 (70%) |
| Carrier | 253 (29%) | 65 (44%) | 86 (69%) | 108 (30%) |
| Amyloid PET, SUVR | 1.42 (1.34, 1.58) | 1.68 (1.39, 2.43) | 2.42 (2.16, 2.70) | 1.42 (1.35, 1.56) |
| Amyloid PET, centiloid | 16 (9, 30) | 40 (14, 106) | 105 (82, 130) | 16 (10, 28) |
| Amyloid PET magnitude stage | | | | |
| $A^{LOW}$ | 564 (65%) | 53 (36%) | 6 (5%) | 231 (65%) |
| $A^{INT}$ | 204 (24%) | 32 (22%) | 18 (15%) | 82 (23%) |
| $A^{HIGH}$ | 96 (11%) | 63 (43%) | 100 (81%) | 42 (12%) |
| Amyloid PET topographic stage | | | | |
| A0 | 491 (57%) | 50 (34%) | 6 (5%) | 199 (56%) |
| A1 | 125 (14%) | 14 (9%) | 1 (1%) | 54 (15%) |
| A2 | 4 (0%) | 3 (2%) | 0 (0%) | 3 (1%) |
| A3 | 26 (3%) | 1 (1%) | 1 (1%) | 9 (3%) |
| A4 | 177 (20%) | 76 (51%) | 115 (93%) | 73 (21%) |
| Indeterminate | 41 (5%) | 4 (3%) | 1 (1%) | 17 (5%) |
| Tau PET, SUVR | 1.19 (1.14, 1.24) | 1.27 (1.19, 1.41) | 1.94 (1.59, 2.26) | 1.20 (1.14, 1.25) |
| Tau PET magnitude stage | | | | |
| $T^{LOW}$ | 752 (87%) | 84 (57%) | 13 (10%) | 303 (85%) |
| $T^{INT}$ | 97 (11%) | 32 (22%) | 9 (7%) | 44 (12%) |
| $T^{HIGH}$ | 15 (2%) | 32 (22%) | 102 (82%) | 8 (2%) |
| Tau PET topographic stage | | | | |
| Braak 0 | 776 (90%) | 81 (55%) | 13 (10%) | 318 (90%) |
| Braak 1–2 | 59 (7%) | 30 (20%) | 8 (6%) | 24 (7%) |
| Braak 3–4 | 11 (1%) | 17 (11%) | 15 (12%) | 7 (2%) |
| Braak 5–6 | 10 (1%) | 18 (12%) | 88 (71%) | 4 (1%) |
| Indeterminate | 8 (1%) | 2 (1%) | 0 (0%) | 2 (1%) |
| Combined amyloid and tau PET stage | | | | |
| None/low severity | 842 (97%) | 112 (76%) | 22 (18%) | 344 (97%) |
| Intermediate/high severity | 16 (2%) | 34 (23%) | 102 (82%) | 9 (3%) |
| Indeterminate | 6 (1%) | 2 (1%) | 0 (0%) | 2 (1%) |
| Plasma $A\beta_{42}/A\beta_{40}$ | 0.061 (0.053, 0.068) | 0.059 (0.050, 0.067) | 0.053 (0.046, 0.059) | 0.060 (0.053, 0.066) |
| Plasma p-tau181, pg/ml | 1.7 (1.3, 2.4) | 2.4 (1.8, 3.5) | 3.7 (3.0, 4.8) | 1.8 (1.4, 2.4) |
| Plasma GFAP, pg/ml | 97 (66, 141) | 135 (93, 181) | 183 (140, 241) | 98 (67, 147) |
| Plasma NfL, pg/ml | 21 (15, 30) | 27 (20, 38) | 33 (25, 40) | 21 (15, 31) |

Among CI participants for tau PET (Fig. 4), p-tau181 was the only single analyte that improved discrimination when added to the base model (C = 0.83 versus 0.77, $P = 0.02$ for Braak 1–2 versus Braak 0; C = 0.85 versus 0.80, $P = 0.03$ for Braak 5–6 versus Braak 3–4). The model with all four plasma analytes often showed improvement in discrimination over the base model (C = 0.84 versus 0.77, $P = 0.02$ for Braak 1–2 versus Braak 0; C = 0.86 versus 0.80, $P = 0.049$ for Braak 5–6 versus Braak 3–4; C = 0.86 versus 0.79, $P = 0.01$ for $T^{HIGH}$ versus $T^{INT}$). The full model also showed improved discrimination over models with $A\beta_{42}/A\beta_{40}$, GFAP or NfL for some of the staging pair comparisons but was not significantly better than discrimination from the p-tau181 models for any of the staging pair comparisons ($P \geq 0.15$). In particular, for Braak 1–2 versus Braak 0, the C statistic from the full model was 0.84 compared to 0.78 ($P = 0.03$) for NfL; for Braak 5–6 versus Braak 3–4, the full model C statistic was 0.86 versus 0.80 ($P = 0.01$) for GFAP and 0.81 ($P = 0.02$) for NfL; for $T^{INT}$ versus $T^{LOW}$, the full model C statistic was 0.75 versus 0.68 ($P = 0.03$) for $A\beta_{42}/A\beta_{40}$, 0.68 ($P = 0.04$) for GFAP and 0.67 ($P = 0.03$) for NfL; and for $T^{HIGH}$ versus $T^{INT}$, the full model C statistic was 0.86 versus 0.79 ($P = 0.01$) for $A\beta_{42}/A\beta_{40}$ and 0.79 ($P = 0.03$) for NfL. None of the plasma analytes alone or in combination significantly improved discrimination over the base model for Braak 3–4 versus Braak 1–2 ($P \geq 0.13$).

When CU and CI participants were combined (Fig. 5), p-tau181 was the only single analyte that improved discrimination when added to the base model (C = 0.85 versus 0.82, $P = 0.004$ for Braak 1–2 versus Braak 0; C = 0.75 versus 0.73, $P = 0.02$ for $T^{INT}$ versus $T^{LOW}$; C = 0.91 versus 0.89, $P = 0.04$ for $T^{HIGH}$ versus $T^{INT}$). The model

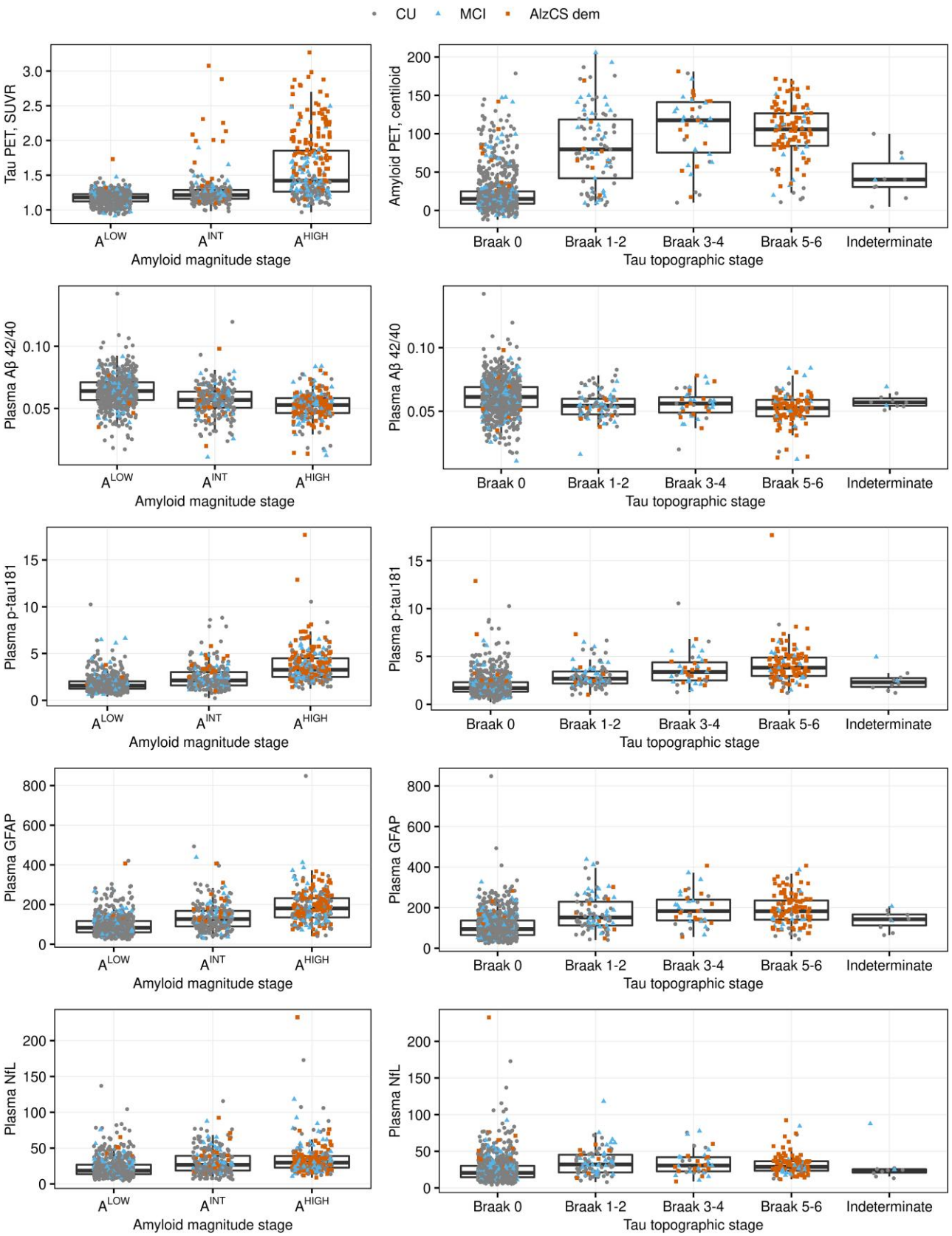


**Figure 2 Box plots of amyloid PET, tau PET and plasma biomarkers by amyloid magnitude stage (*left*) and tau PET topographic stage (*right*).**

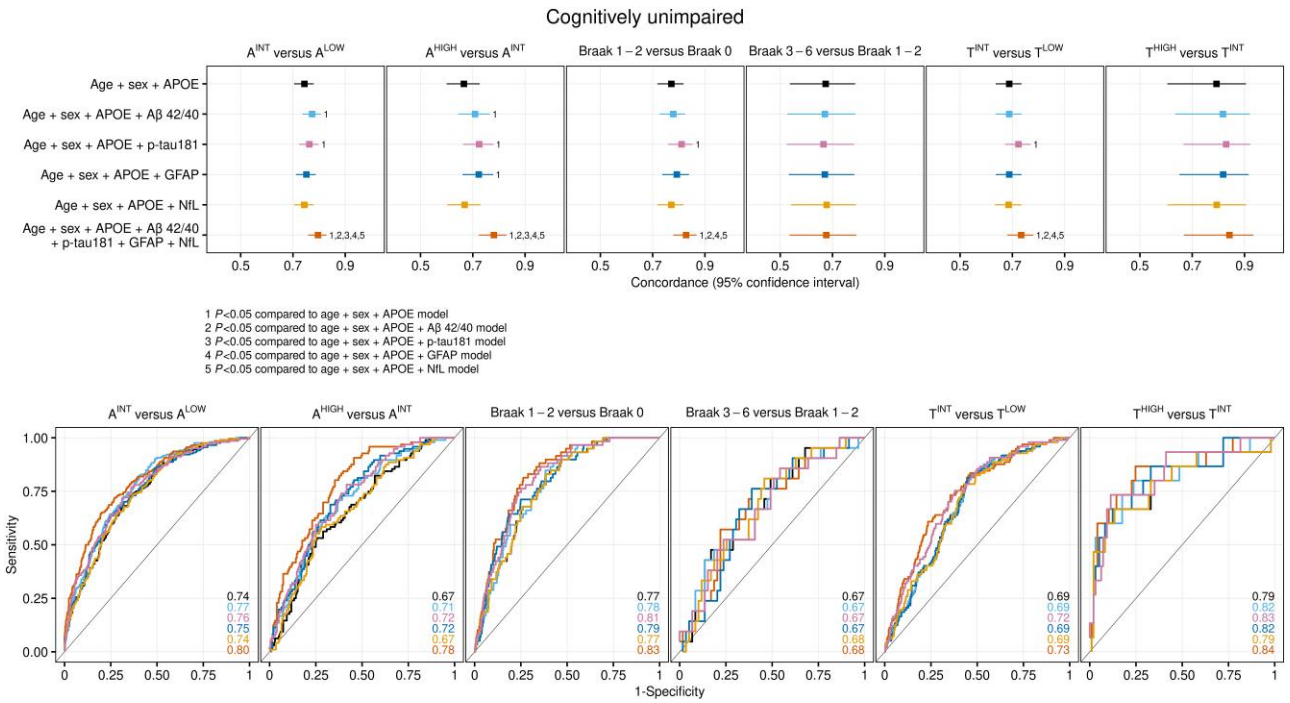


**Figure 3 Discrimination between lower and higher PET stage pairs among CU participants for several models including plasma analyte(s) as predictors as well as a base model with risk variables.** Concordance (95% confidence interval) estimates from multinomial regression models fit among CU participants are shown on the *top row* (forest plots) and ROC curves for the same models are shown in the *bottom row*. The colours in the forest plots in the *top row* for each model match the corresponding colours of the ROC curves in the *bottom row*. The numbers in the *bottom right* of each ROC plot represent the C statistic estimate from the corresponding forest plot above it. Separate models were fit for the amyloid PET magnitude stage outcome, the tau PET topographic stage outcome and the tau PET magnitude stage outcome. The columns represent different contrasts between the PET stages. Braak 3–4 and Braak 5–6 were combined due to small numbers in these groups among the CU participants. Models were compared to answer the following: (i) how well does each plasma analyte discriminate among amyloid PET and tau PET stages when added individually to a base model consisting of risk factors? and (ii) is discrimination between PET stages improved over the base model or models with individual analytes plus base when all plasma analytes were included in the model simultaneously? Footnotes below the *top row* show which comparisons were significantly different with $P < 0.05$.

with all four plasma analytes often showed improvement in discrimination over the base model (C = 0.86 versus 0.82, $P < 0.001$ for Braak 1–2 versus Braak 0; C = 0.81 versus 0.77, $P = 0.04$ for Braak 3–4 versus 1–2; C = 0.76 versus 0.73, $P = 0.003$ for $T^{INT}$ versus $T^{LOW}$; C = 0.92 versus 0.89, $P = 0.02$ for $T^{HIGH}$ versus $T^{INT}$). The full model also showed improved discrimination over models with $A\beta_{42}/A\beta_{40}$, GFAP or NfL for some of the staging pair comparisons, but was not significantly better than discrimination from the p-tau181 models for any of the staging pair comparisons ($P \geq 0.06$). None of the plasma analytes alone or in combination significantly improved discrimination over the base model for Braak 5–6 versus Braak 3–4 ($P \geq 0.14$).

## Predicting a PET proxy of intermediate/high severity of neuropathological change with plasma biomarkers

Among CU individuals, discrimination between a PET proxy of intermediate/high severity versus none/low severity was similar across most models; the model with all four plasma biomarkers plus base (C = 0.88) improved discrimination compared to the model with GFAP plus base (C = 0.85, $P = 0.01$; Fig. 6). Among CI individuals, the models with p-tau181 (C = 0.90, $P < 0.001$) and GFAP (C = 0.86, $P < 0.001$) improved discrimination over the base model alone (C = 0.78). When all four analytes were included in the model, discrimination was similar to the model with p-tau181 (C = 0.91 versus 0.90, $P = 0.18$). Among all participants, the base model provided excellent discrimination between intermediate/high severity versus none/low severity (C = 0.95). Adding p-tau181 individually (C = 0.96, $P < 0.001$) or all four analytes (C = 0.97, $P = 0.001$) to the base model improved discrimination. Detailed odds ratios from all models are found in Supplementary Tables 6 and 7.

## Predicting amyloid and PET stages in Quanterix plasma biomarkers without base risk factors

When evaluating the plasma biomarkers without adjusting for base risk factors, none of the individual biomarkers improved prediction of PET stages compared to the base risk factor models in CU, CI or all participants. However, among CU and among CI participants, the model with all four plasma biomarkers combined but no base risk factors did improve prediction of $A^{HIGH}$ versus $A^{INT}$ stages compared to the base model and all models with individual biomarkers (C = 0.77 versus 0.59–0.70, $P \leq 0.01$ for CU; C = 0.81 versus 0.56–0.72, $P \leq 0.03$ for CI; Supplementary Figs 5–7 and Supplementary Tables 3–5). Among CI participants, the model with all four biomarkers also improved prediction of intermediate/high severity versus none/low compared to the base model and all models with individual biomarkers (C = 0.87 versus 0.50–0.81, $P \leq 0.009$; Supplementary Fig. 8 and Supplementary Tables 6 and 7).

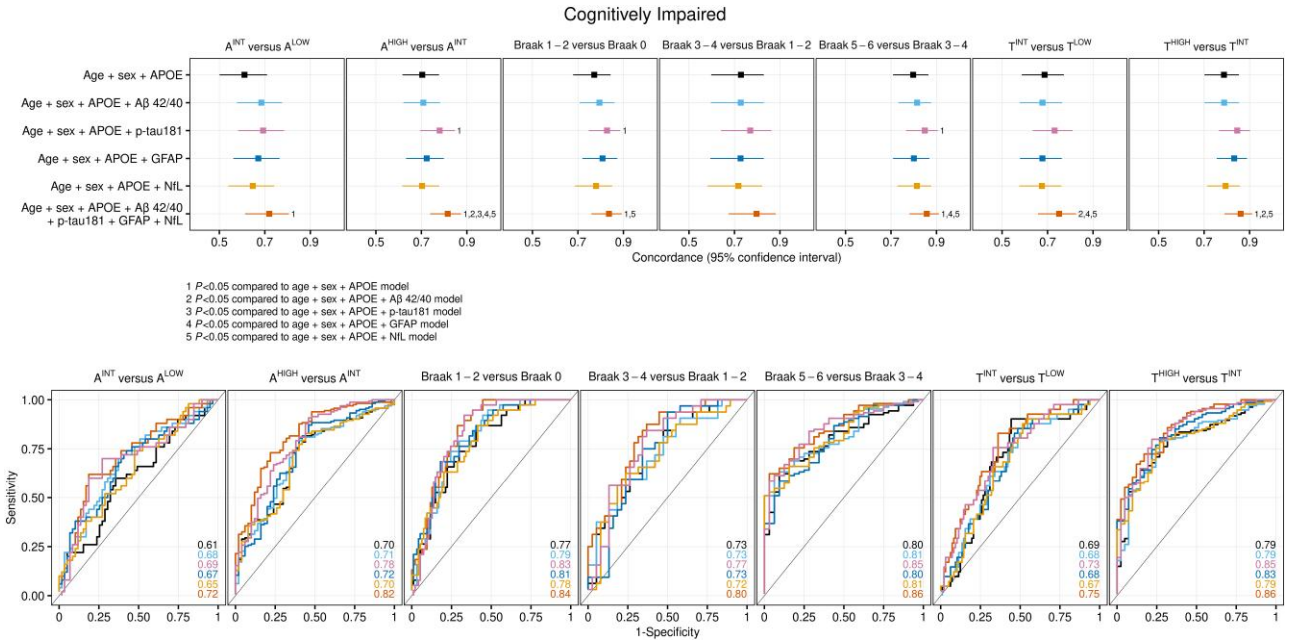


**Figure 4 Discrimination between lower versus higher PET stage pairs among CI participants for several models including plasma analyte(s) as predictors as well as a base model with risk variables.** Concordance (95% confidence interval) estimates from multinomial regression models fit among CI participants are shown on the *top row* (forest plots) and ROC curves for the same models are shown in the *bottom row*. The colours in the forest plots in the *top row* for each model match the corresponding colours of the ROC curves in the *bottom row*. The numbers in the *bottom right* of each ROC plot represent the C statistic estimate from the corresponding forest plot above it. Separate models were fit for the amyloid PET magnitude stage outcome, the tau PET topographic stage outcome and the tau PET magnitude stage outcome. The columns represent different contrasts between the PET stages. Models were compared to answer the following: (i) how well does each plasma analyte discriminate among amyloid PET and tau PET stages when added individually to a base model consisting of risk factors? and (ii) is discrimination between PET stages improved over the base model or models with individual analytes plus base when all plasma analytes were included in the model simultaneously? Footnotes below the *top row* show which comparisons were significantly different with $P < 0.05$.

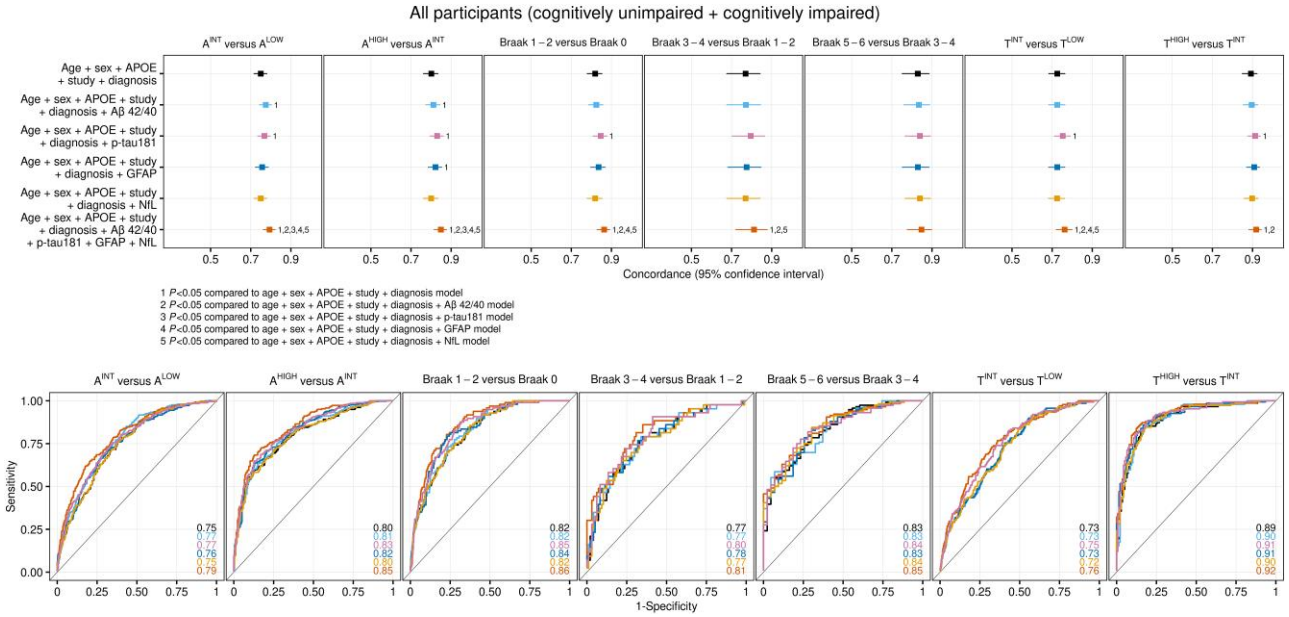


**Figure 5 Discrimination between lower versus higher PET stage pairs among all participants (CU and CI) for several models including plasma analyte(s) as predictors as well as a base model with risk variables.** Concordance (95% confidence interval) estimates from multinomial regression models fit among all participants are shown on the *top row* (forest plots) and ROC curves for the same models are shown in the *bottom row*. The colours in the forest plots in the *top row* for each model match the corresponding colours of the ROC curves in the *bottom row*. The numbers in the *bottom right* of each ROC plot represent the C statistic estimate from the corresponding forest plot above it. Separate models were fit for the amyloid PET magnitude stage outcome, the tau PET topographic stage outcome and the tau PET magnitude stage outcome. The columns represent different contrasts between the PET stages. Models were compared to answer the following: (i) how well does each plasma analyte discriminate among amyloid PET and tau PET stages when added individually to a base model consisting of risk factors? and (ii) is discrimination between PET stages improved over the base model or models with individual analytes plus base when all plasma analytes were included in the model simultaneously? Footnotes below the *top row* show which comparisons were significantly different with $P < 0.05$. The risk factor model included age, sex, APOE genotype, a three-level study and clinical diagnosis variable (MCSA CU, MCSA CI, ADRC CI) and an interaction with age and the study/clinical diagnosis variable.

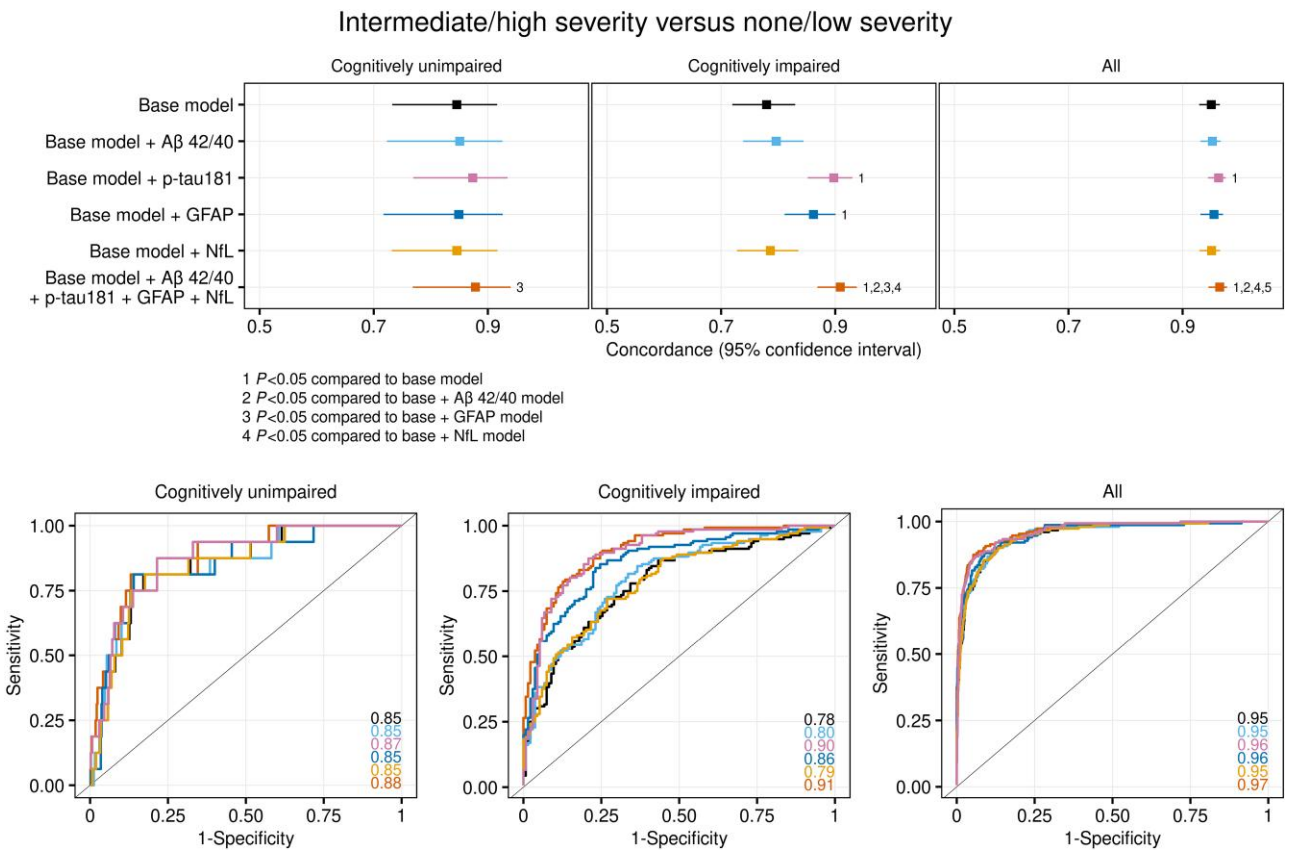


**Figure 6 Discrimination between a combined amyloid and tau PET stage as a proxy of intermediate/high versus none/low Alzheimer's disease neuropathologic change among CU, CI and all participants for models including plasma analyte(s) as predictors and a base model with risk variables.** Concordance (95% confidence interval) estimates from logistic regression models fit among CU (*left*), CI (*middle*) and all participants (*right*) are shown in the *top row* and ROC curves for the same models are shown in the *bottom row*. The numbers in the *bottom right* of each ROC plot represent the C statistic estimate from the corresponding forest plot above it. Models were compared to answer the following: (i) how well does each plasma analyte discriminate among the combined amyloid and tau PET stage when added individually to a base model consisting of risk factors? and (ii) is discrimination between PET stages improved over the base model or models with individual analytes plus base when all plasma analytes were included in a model simultaneously? Footnotes below the *top row* show which comparisons were significantly different with $P < 0.05$. The base model for the CU and CI models included age, sex and APOE genotype. The base model for the models fit among all participants included age, sex, APOE genotype, a three-level study and clinical diagnosis variable (MCSA CU, MCSA CI, ADRC CI) and an interaction with age and the study/clinical diagnosis variable.

### Predicting amyloid and tau PET stages in the subset with Lilly plasma p-tau217

Median Quanterix p-tau181 and Lilly p-tau217 both increased with higher amyloid magnitude stage and tau topographic stage in the subset of CU participants with both p-tau biomarkers (Supplementary Fig. 9). Lilly p-tau217 plus base risk factors improved discrimination of $A^{HIGH}$ versus $A^{INT}$ compared to Quanterix p-tau181 plus base (C = 0.85 versus 0.74, $P = 0.004$) but not compared to all four Quanterix biomarkers plus base (C = 0.83, $P = 0.49$; Fig. 7). For $A^{INT}$ versus $A^{LOW}$, the model with all four Quanterix plasma biomarkers plus base (C = 0.84) improved discrimination over the models with either Quanterix p-tau181 (C = 0.79, $P < 0.001$) or Lilly p-tau217 individually plus base (C = 0.80, $P = 0.01$). C statistics were more similar for the models with either Quanterix p-tau181, Lilly p-tau217 or all four Quanterix biomarkers for Braak 1–6 versus Braak 0 or $T^{HIGH/INT}$ versus $T^{LOW}$. When evaluating the biomarkers without adjusting for base risk factors, the results were similar for $A^{HIGH}$ versus $A^{INT}$; Lilly p-tau217 improved discrimination of $A^{HIGH}$ versus $A^{INT}$ compared to Quanterix p-tau181 (C = 0.85 versus 0.73, $P = 0.006$) but not compared to the model with all four Quanterix markers (C = 0.83, $P = 0.55$; Supplementary Fig. 10). Neither Lilly p-tau217 nor Quanterix p-tau181 individually improved discrimination compared to the base risk factor model for the other PET stages. Detailed odds ratios from all models are found in Supplementary Table 8.

## Discussion

We examined approaches for staging amyloid PET and tau PET and then determined how well plasma analytes alone or in combination could discriminate between PET stages. We found that models with individual Quanterix analytes (most often p-tau181) along with base risk factors discriminated most amyloid PET and tau PET stages. However, for both unimpaired, impaired and all participants combined, p-tau181 or the combination of all four Quanterix plasma analytes plus base most often provided the best discrimination among amyloid and tau PET stages (C statistics in the acceptable to excellent range). Discriminating a PET proxy of intermediate/high from low/none severity of Alzheimer's disease

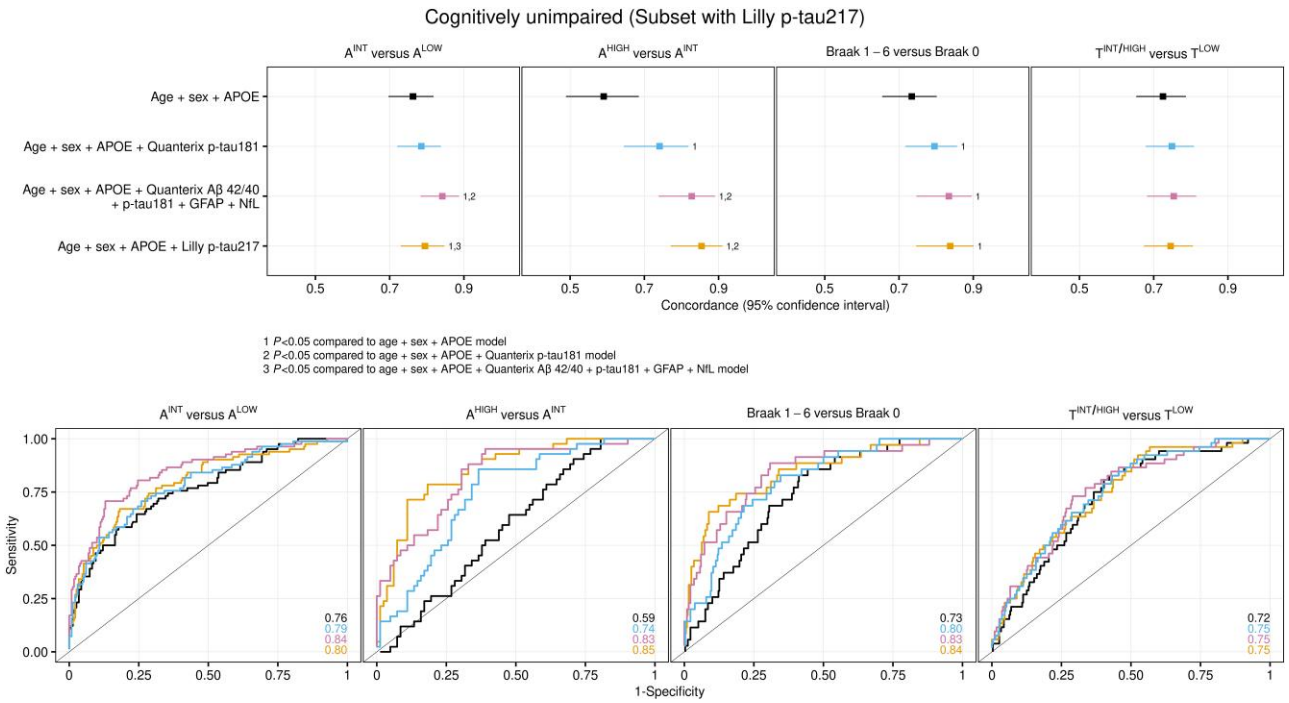


**Figure 7 Discrimination between lower and higher PET stage pairs among the subset of CU participants with Lilly plasma p-tau217 for several models including plasma analyte(s) as predictors as well as a base model with risk variables.** Concordance (95% confidence interval) estimates from multinomial regression models fit among the subset of CU participants with Lilly p-tau217 data are shown on the *top row* (forest plots) and ROC curves for the same models are shown in the *bottom row*. The colours in the forest plots in the *top row* for each model match the corresponding colours of the ROC curves in the *bottom row*. The numbers in the *bottom right* of each ROC plot represent the C statistic estimate from the corresponding forest plot above it. Separate models were fit for the amyloid PET magnitude stage outcome, the tau PET topographic stage outcome and the tau PET magnitude stage outcome. The columns represent different contrasts between the PET stages. $T^{INT}$ and $T^{HIGH}$ were combined and Braak 1–2, 3–4 and 5–6 were combined due to small numbers in these groups among CU in the Lilly subset. Models were compared to answer the following: (i) how well does Quanterix p-tau181, Lilly p-tau217, and the combination of all four Quanterix biomarkers discriminate among amyloid PET and tau PET stages when added to a base model consisting of risk factors? (ii) is discrimination between PET stages improved when using Lilly p-tau217 added to the base model compared to Quanterix p-tau181 added to the base model? and (iii) is discrimination between PET stages improved when using Lilly p-tau217 added to the base model compared to a model with all Quanterix plasma analytes plus the base model? Footnotes below the *top row* show which comparisons were significantly different with $P < 0.05$.

neuropathological change with all four Quanterix plasma analytes plus base was excellent for CU (C = 0.88), CI (C = 0.91) and combined (C = 0.97) participants, but was not appreciably better than a model with p-tau181 alone (C = 0.87 for CU, C = 0.90 for CI, C = 0.96 for all). In the Lilly CU subset, the Lilly p-tau217 assay outperformed the Quanterix p-tau181 assay for $A^{HIGH}$ versus $A^{INT}$ (C = 0.85 versus 0.74) but was comparable to all four Quanterix assays combined (C = 0.83). For other PET stages, the Lilly p-tau217 and Quanterix p-tau181 performed similarly. For $A^{INT}$ versus $A^{LOW}$ the model with all four Quanterix assays improved discrimination over both Lilly p-tau217 and Quanterix p-tau181 (C = 0.84 versus 0.80 and 0.79).

## Amyloid PET staging

The lower cut-off point we used for amyloid PET magnitude staging, centiloid 22, is within the centiloid range (19–25) that has been identified as a useful detection limit threshold by different methods: reliable worsening in rate of amyloid accumulation,[61] the neuropathologically determined boundary between Thal phase 1 and phase 2[76] and the cut-off point between pathologically determined CERAD (Consortium to Establish a Registry for Alzheimer's Disease) intermediate-to-high Alzheimer's disease neuropathological change.[77] The upper cut-off point, centiloid 68, does not correspond to a neuropathologically established milestone but is the value we found to represent the apex of the amyloid PET rate of change versus SUVR function.[44,78]

## Tau PET staging

Very few CU participants were in Braak 3–4 or Braak 5–6 stage. This is consistent with the explanation that higher neocortical tau PET burden is incompatible with preserved cognitive capability in most people.[79–81]

We implemented both a topographic and a magnitude staging scheme for tau PET. Many studies that have examined tau PET staging, as opposed to binary normal versus abnormal, have mirrored Braak neuropathological staging.[51–60] Compressing the six Braak neuropathological stages into four as we have done has an established precedent in the neuropathology and tau PET literature.[82]

We also employed a magnitude staging scheme for tau PET. Topographic staging operates from the assumption that tau spreads via a single topographic progression pattern in all people. Some recent data have challenged this assumption, however, and assert that while the standard Braak pattern may be the most common, it is not an obligate progression pattern in all people.[83–85] We and others have demonstrated that the temporal lobe meta-region of interest we used for magnitude tau PET staging includes areas that are invariably involved even in persons

with atypical Alzheimer's disease phenotypes.[81,86–88] The lower cut-off point we used for magnitude tau PET staging (SUVR 1.29) was defined using a neuropathological standard and corresponds to the SUVR value separating Braak 4 or greater from less than Braak 4.[74,76] The higher cut-off point (SUVR 1.43) does not have an established neuropathological basis and was based in part on the topographic staging analysis where SUVR 1.43 fell at the lower quartile of the Braak 3–4 group, separating this group from Braak 1–2 (Fig. 1).

## Predicting amyloid PET stage with plasma biomarkers

Prior studies have examined how well a single plasma analyte, typically p-tau 181 or 217, or $A\beta_{42}/A\beta_{40}$ predicts normal versus abnormal amyloid PET[2,4,7–10,20,21,36,89–94] or correlates with amyloid PET on a continuous basis.[7–9,20,21,23,91–93,95] One study, Mila-Aloma *et al.*,[6] did examine the ability of individual plasma analytes plus risk factors to discriminate between amyloid PET centiloid values greater versus less than 12 and greater versus less than 30. These results are not directly comparable to ours, however, because the thresholds we used for staging were quite different. Centiloid 12 lies below the value we have calculated to be reliably detectable[61] and centiloid 30 lies well below the value seen in individuals with MCI or AlzCS dem and abnormal amyloid PET.[96]

In prior studies where the ability to discriminate normal versus abnormal amyloid PET has been compared between individual plasma analytes versus combinations of analytes, combinations have performed slightly better.[8,21,31,97] For example, Janelidze *et al.*[8] reported an AUC of 0.80 for plasma p-tau181 alone and 0.77 for $A\beta_{42}/A\beta_{40}$ alone, compared with 0.85 when the two were combined. Chatterjee *et al.*[31] also found that combinations of plasma biomarkers more accurately discriminated between unimpaired individuals with normal versus abnormal amyloid than individual analytes with best AUCs over 0.90. These results are better than our findings in CU participants for amyloid staging. An obvious explanation is that discriminating among stages of amyloid PET is a more difficult diagnostic task than binary discrimination of normal versus abnormal. Nonetheless, our findings support our initial supposition that combinations of plasma biomarkers are more accurate for discriminating amyloid PET stages than individual plasma analytes.

## Predicting tau PET stage with plasma biomarkers

Prior studies have examined how well a single p-tau analyte discriminates tau PET scored in a binary manner (normal versus abnormal)[6,8–10,30,90,92,98] or correlates with continuous tau PET measures in defined regions of interest.[8,9,20,30,92,93,95] We are not aware of other work using all the plasma analytes we did to discriminate tau PET stages. Janelidze *et al.*[8] and Karikari *et al.*[9] examined if a combination of p-tau181 and $A\beta_{42}/A\beta_{40}$ predicted abnormal tau PET status in different Braak regions of interest, but this is different from discriminating people in different Braak stages. Janelidze *et al.*[8] and Karikari *et al.*[9] also examined the ability of p-tau181 to separate groups defined by different Braak tau PET stages and AUCs were in the 0.80–0.96 range. However, our results are not directly comparable because CU, MCI, AlzCS dem and participants with non-Alzheimer's disease neurodegenerative diseases were combined in those analyses,[8,9] whereas we did not include non-Alzheimer's disease neurodegenerative diseases and our primary analyses were performed separately in CU and CI participants.

For both CU, CI and all participants, the models with all four analytes most often had the highest C statistic, but the discrimination using all four analytes was not appreciably better than when using only the p-tau181 analyte. This is different from amyloid PET staging, where the model with all four analytes plus base risk predictors was usually superior to the model with p-tau181 individually plus base. Another interesting finding was that plasma biomarkers did discriminate between intermediate versus none/low tau PET stages but not between high versus intermediate tau PET stages in CU participants, whereas plasma biomarkers discriminated between both intermediate versus none/low and high versus intermediate among CI participants. This may simply reflect the nature of the relationship between tau and symptoms; few CUs have a high neocortical tau burden.[79–81] Therefore, we lack power to discriminate between high versus intermediate tau in CUs.

## Secondary analyses

In the analyses with CU and CI combined, the performance of plasma biomarkers for discriminating between most amyloid and tau PET stages was similar to the performance among the individual subsets of CU or CI participants for the models with all four biomarkers. The base risk factor models had higher C statistics in the combined group for several models, likely because clinical diagnosis was included. We focus on analyses of CU and CI participants separately rather than combined because for all scenarios we can envision (clinical care and clinical trials); the context of use would be different for an unimpaired versus an impaired individual. Thus, the most clinically relevant data would be those in CU and CI separately.

We also performed modelling with plasma biomarkers alone, without base risk factors. However, we believe that including risk factor variables in the models is the best way to account for differences in the distribution of age, sex and APOE across cohorts in different studies. Not adjusting for these variables could lead to erroneous conclusions that differences in biomarker performance between studies were attributable to biomarker characteristics alone rather than being due in part (perhaps in large part) to inter-study differences in the distributions of risk factors.

## Predicting a PET proxy of intermediate/high severity of neuropathological change with plasma biomarkers

The most widely accepted method for evaluating Alzheimer's disease neuropathological change incorporates staging of both Aβ plaque and tau neurofibrillary tangle pathology.[82] Intermediate or high Alzheimer's disease neuropathological change is regarded as sufficient to produce dementia[82] and can be summarized as the conjunction of moderate to severe neuritic plaques, Thal phase 2 or greater and neocortical tangles (Braak 3 or greater). While PET is not as sensitive as direct tissue examination,[99] imaging–autopsy correlation studies have shown that persons with the conjunction of $>A^{LOW}$ and >Braak 1–2, as we have defined them with amyloid and tau PET, would meet neuropathological criteria for moderate to severe Alzheimer's disease neuropathological change.[56,74,76,77,99–105] Discrimination of this PET proxy of intermediate/high severity versus none/low severity of Alzheimer's disease neuropathological change was excellent when using all four analytes in CU (C = 0.88), CI (C = 0.91) and all (C = 0.97) participants. However, the discrimination was not appreciably better than the model with p-tau181 (C = 0.87, 0.90 and 0.96, respectively). The ability to identify individuals

who would likely qualify for a neuropathological diagnosis of Alzheimer's disease using plasma biomarkers could have utility for clinical trials and neurological practice.

### Lilly p-tau 217 subset

In prior head-to-head comparisons, Quanterix $A\beta_{42}/A\beta_{40}$ and p-tau181 have not performed as well as other in-class assays.[5,106] For this reason, we performed an analysis using the Lilly p-tau217 assay, which has performed as well as or better than any p-tau immunoassay, with superior performance only found with a mass spectrometry p-tau occupancy assay.[106] As expected, the performance of the Lilly p-tau217 assay was as good or slightly better than the Quanterix p-tau181; this difference was significant for discriminating $A^{HIGH}$ versus $A^{INT}$. However, the model with all four Quanterix biomarkers was similar or slightly better than the Lilly p-tau217 assay for all PET staging outcomes.

### Limitations

Head-to-head comparisons have shown that individual assays with better diagnostic performance than the Quanterix analytes used in this study exist for both plasma $A\beta_{42}/A\beta_{40}$ and p-tau.[5,10,21,90,107,108] Modest diagnostic performance is illustrated by the overlap in individual plasma values across clinical diagnostic groups (Table 1) and across PET stages (Fig. 2). Modest diagnostic performance is also illustrated by the fact that discriminating among most amyloid and tau PET stages by individual Quanterix analytes without the base risk factors was not more effective than with the base risk factors alone (Supplementary Figs 5–8). However, the Quanterix platform used in this study is one of only two that are both currently commercially available and where all the plasma analytes we examined can be run on the same platform.

While precedent exists in the PET and neuropathological literature for both the amyloid and tau PET staging schemes we used, an argument can always be raised that a different staging scheme or different cut-off points might have given different results. Some PET staging schemes have employed more fine-grained stages in comparison to the approach we used. However, more granular staging would have resulted in an unwieldly number of pairwise comparisons for staging discrimination with plasma biomarkers. In addition, the tau PET ligand we used may not have optimal sensitivity/specificity needed to accurately discriminate uptake in small medial temporal regions needed for early Braak-like staging.[52,109] Furthermore, off-target uptake in the choroid plexus with this tau PET tracer may interfere with hippocampal measures; thus, the hippocampus, which is important in discriminating early Braak neuropathological stages, was not included in our tau PET staging.

## Conclusions

Plasma analytes can provide useful predictive information about the stage of both amyloid and tau PET, although for many staging comparisons the incremental value plasma biomarkers add beyond risk factor predictors was modest. For amyloid PET, the combination of all four Quanterix plasma analytes was better than single analytes for most staging predictions, whereas for tau PET and the combined amyloid and tau PET proxy of Alzheimer's disease neuropathological change, the combination of all four plasma analytes had similar prediction ability compared with only using the p-tau181 analyte. In head-to-head comparisons, the Lilly p-tau217 assay performed similarly or better than the Quanterix p-tau181 assay. However, using all four Quanterix biomarkers performed similarly or better than the Lilly p-tau217 assay. Staging both amyloid and tau pathology may become more important as clinical trials focus on interventions targeted to more specific stages of Alzheimer's disease.

## Acknowledgements

The Alexander Family Alzheimer's Disease Research Professorship of the Mayo Clinic.

## Funding

Funding was provided by the National Institutes of Health (R37 AG011378, RO1 AG041851, R01 AG056366, R01 NS097495, U01 AG06786, R01 AG034676) and the GHR Foundation. Funders had no role in design and conduct of the study; collection, management, analysis and interpretation of the data; preparation, review or approval of the manuscript; and decision to submit the manuscript for publication. The corresponding author had full access to all the data in the study and takes responsibility for the integrity of the data and the accuracy of the data analysis.

## Competing interests

C.R.J. receives funding from the NIH and the Alexander Family Alzheimer's Disease Research Professorship of the Mayo Clinic. A.A.-S. has participated in advisory boards for Roche Diagnostics, Fujirebio Diagnostics and Siemens Healthineers. B.F.B. receives honoraria for SAB activities for the Tau Consortium; grant support for clinical trials from Alector, Biogen, Transposon, Cognition Therapeutics, GE Healthcare; and grant support from the NIH, Lewy Body Dementia Association, American Brain Foundation and Little Family Foundation Professorship. K.K. received research support from Avid Radiopharmaceuticals, Eli Lilly and consults for Biogen. She is supported by the NIH. T.M.T. receives NIH support (C.R.J.'s grant). M.M.M. receives research support from the NIH and DOD and has consulted for Biogen, Brain Protection Company, LabCorp, Lilly, Merck, Roche, Siemens Healthineers and Sunbird Bio. D.S.K. serves on a Data Safety Monitoring Board for the Dominantly Inherited Alzheimer Network Treatment Unit study. He served on a Data Safety Monitoring Board for a tau therapeutic for Biogen (until 2021) but received no personal compensation. He is an investigator in clinical trials sponsored by Biogen, Lilly Pharmaceuticals and the University of Southern California. He has served as a consultant for Roche, Samus Therapeutics, Magellan Health, Biovie and Alzeca Biosciences but receives no personal compensation. He attended an Eisai advisory board meeting for lecanemab on 2 December 2022, but received no compensation. He receives funding from the NIH. J.G.-R. receives funding from the NIH. He is an investigator in clinical trials sponsored by Biogen, Eisai and the University of Southern California. V.J.L. consults for Bayer Schering Pharma, Piramal Life Sciences, Eisai, Inc., AVID Radiopharmaceuticals and Merck Research, and receives research support from GE Healthcare, Siemens Molecular Imaging, AVID Radiopharmaceuticals and the NIH (NIA, NCI). P.V. receives funding from the NIH. C.G.S. receives funding from the NIH. R.C.P. has consulted for Roche, Inc.; Genentech, Inc.; Eli Lilly, Inc.; Nestle, Inc. and Eisai, Inc.; a DSMB for Genentech, Inc. and receives royalties from Oxford University Press for Mild Cognitive Impairment and from UpToDate. His research funding is from NIH/NIA. The other authors report no competing interests.

## Supplementary material

Supplementary material is available at *Brain* online.

## References


1. Ovod V, Ramsey KN, Mawuenyega KG, *et al*. Amyloid beta concentrations and stable isotope labeling kinetics of human plasma specific to central nervous system amyloidosis. *Alzheimers Dement*. 2017;13:841-849.
2. Nakamura A, Kaneko N, Villemagne VL, *et al*. High performance plasma amyloid-β biomarkers for Alzheimer's disease. *Nature*. 2018;554:249-254.
3. Nabers A, Perna L, Lange J, *et al*. Amyloid blood biomarker detects Alzheimer's disease. *EMBO Mol Med*. 2018;10:e8763.
4. Schindler SE, Bollinger JG, Ovod V, *et al*. High-precision plasma beta-amyloid 42/40 predicts current and future brain amyloidosis. *Neurology*. 2019;93:e1647-e1659.
5. Janelidze S, Teunissen CE, Zetterberg H, *et al*. Head-to-head comparison of 8 plasma amyloid-beta 42/40 assays in Alzheimer disease. *JAMA Neurol*. 2021;78:1375-1382.
6. Mila-Aloma M, Ashton N, Shekari M, *et al*. Plasma p-tau231 and p-tau217 as state markers of amyloid-β pathology in preclinical Alzheimer's disease. *Nat Med*. 2022;28:1797-1801.
7. Li G, Sokal I, Quinn JF, *et al*. CSF tau/Abeta42 ratio for increased risk of mild cognitive impairment: A follow-up study. *Neurology*. 2007;69:631-639.
8. Janelidze S, Mattsson N, Palmqvist S, *et al*. Plasma P-tau181 in Alzheimer's disease: Relationship to other biomarkers, differential diagnosis, neuropathology and longitudinal progression to Alzheimer's dementia. *Nat Med*. 2020;26:379-386.
9. Karikari TK, Pascoal TA, Ashton NJ, *et al*. Blood phosphorylated tau 181 as a biomarker for Alzheimer's disease: A diagnostic performance and prediction modelling study using data from four prospective cohorts. *Lancet Neurol*. 2020;19:422-433.
10. Palmqvist S, Janelidze S, Quiroz YT, *et al*. Discriminative accuracy of plasma phospho-tau217 for Alzheimer disease vs other neurodegenerative disorders. *JAMA Neurol*. 2020;324:772-781.
11. Thijssen EH, La Joie R, Wolf A, *et al*. Diagnostic value of plasma phosphorylated tau181 in Alzheimer's disease and frontotemporal lobar degeneration. *Nat Med*. 2020;26:387-397.
12. Karikari TK, Benedet AL, Ashton NJ, *et al*. Diagnostic performance and prediction of clinical progression of plasma phospho-tau181 in the Alzheimer's disease neuroimaging initiative. *Mol Psychiatry*. 2021;26:429-442.
13. Palmqvist S, Tideman P, Cullen N, *et al*. Prediction of future Alzheimer's disease dementia using plasma phospho-tau combined with other accessible measures. *Nat Med*. 2021;27:1034-1042.
14. Pichet Binette A, Palmqvist S, Bali D, *et al*. Combining plasma phospho-tau and accessible measures to evaluate progression to Alzheimer's dementia in mild cognitive impairment patients. *Alzheimers Res Ther*. 2022;14:46.
15. Therriault J, Benedet AL, Pascoal TA, *et al*. Association of plasma p-tau181 with memory decline in non-demented adults. *Brain Commun*. 2021;3:fcab136.
16. Janelidze S, Berron D, Smith R, *et al*. Associations of plasma phospho-Tau217 levels with tau positron emission tomography in early Alzheimer disease. *JAMA Neurol*. 2021;78:149-156.
17. Moscoso A, Grothe MJ, Ashton NJ, *et al*. Longitudinal associations of blood phosphorylated Tau181 and neurofilament light chain with neurodegeneration in Alzheimer disease. *JAMA Neurol*. 2021;78:396-406.
18. Moscoso A, Grothe MJ, Ashton NJ, *et al*. Time course of phosphorylated-tau181 in blood across the Alzheimer's disease spectrum. *Brain*. 2021;144:325-339.
19. Pilotto A, Parigi M, Bonzi G, *et al*. Differences between plasma and cerebrospinal fluid p-tau181 and p-tau231 in early Alzheimer's disease. *J Alzheimers Dis*. 2022;87:991-997.
20. Mielke MM, Hagen CE, Xu J, *et al*. Plasma phospho-tau181 increases with Alzheimer's disease clinical severity and is associated with tau- and amyloid-positron emission tomography. *Alzheimers Dement*. 2018;14:989-997.
21. Brickman AM, Manly JJ, Honig LS, *et al*. Plasma p-tau181, p-tau217, and other blood-based Alzheimer's disease biomarkers in a multi-ethnic, community study. *Alzheimers Dement*. 2021;17:1353-1364.
22. Mielke MM, Dage JL, Frank RD, *et al*. Performance of plasma phosphorylated tau 181 and 217 in the community. *Nat Med*. 2022;28:1398-1405.
23. Mattsson-Carlgren N, Janelidze S, Bateman RJ, *et al*. Soluble P-tau217 reflects amyloid and tau pathology and mediates the association of amyloid with tau. *EMBO Mol Med*. 2021;13:e14022.
24. Morrison MS, Aparicio HJ, Blennow K, *et al*. Antemortem plasma phosphorylated tau (181) predicts Alzheimer's disease neuropathology and regional tau at autopsy. *Brain*. 2022;145:3546-3557 .
25. Smirnov DS, Ashton NJ, Blennow K, *et al*. Plasma biomarkers for Alzheimer's disease in relation to neuropathology and cognitive change. *Acta Neuropathol*. 2022;143:487-503.
26. Mielke MM, Syrjanen JA, Blennow K, *et al*. Plasma and CSF neurofilament light: Relation to longitudinal neuroimaging and cognitive measures. *Neurology*. 2019;93:e252-e260.
27. Mattsson N, Andreasson U, Zetterberg H, Blennow K. Association of plasma neurofilament light with neurodegeneration in patients with Alzheimer disease. *JAMA Neurol*. 2017;74:557-566.
28. Mattsson N, Cullen NC, Andreasson U, Zetterberg H, Blennow K. Association between longitudinal plasma neurofilament light and neurodegeneration in patients with Alzheimer disease. *JAMA Neurol*. 2019;76:791-799.
29. Ashton NJ, Hye A, Rajkumar AP, *et al*. An update on blood-based biomarkers for non-Alzheimer neurodegenerative disorders. *Nat Rev Neurol*. 2020;16:265-284.
30. Mattsson-Carlgren N, Janelidze S, Palmqvist S, *et al*. Longitudinal plasma p-tau217 is increased in early stages of Alzheimer's disease. *Brain*. 2020;143:3234-3241.
31. Chatterjee P, Pedrini S, Ashton NJ, *et al*. Diagnostic and prognostic plasma biomarkers for preclinical Alzheimer's disease. *Alzheimers Dement*. 2022;18:1141-1154.
32. Teunissen CE, Verberk IMW, Thijssen EH, *et al*. Blood-based biomarkers for Alzheimer's disease: Towards clinical implementation. *Lancet Neurol*. 2022;21:66-77.
33. Benedet AL, Leuzy A, Pascoal TA, *et al*. Stage-specific links between plasma neurofilament light and imaging biomarkers of Alzheimer's disease. *Brain*. 2020;143:3793-3804.
34. Verberk IMW, Laarhuis MB, van den Bosch KA, *et al*. Serum markers glial fibrillary acidic protein and neurofilament light for prognosis and monitoring in cognitively normal older people: A prospective memory clinic-based cohort study. *Lancet Healthy Longev*. 2021;2:e87-e95.
35. Abdelhak A, Foschi M, Abu-Rumeileh S, *et al*. Blood GFAP as an emerging biomarker in brain and spinal cord disorders. *Nat Rev Neurol*. 2022;18:158-172.
36. Thijssen EH, Verberk IMW, Kindermans J, *et al*. Differential diagnostic performance of a panel of plasma biomarkers for different types of dementia. *Alzheimers Dement (Amst)*. 2022;14:e12285.

37. O'Connor A, Abel E, Benedet AL, *et al*. Plasma GFAP in presymptomatic and symptomatic familial Alzheimer's disease: A longitudinal cohort study. *J Neurol Neurosurg Psychiatry*. 2023;94: 90-92.
38. Pereira JB, Janelidze S, Smith R, *et al*. Plasma GFAP is an early marker of amyloid-beta but not tau pathology in Alzheimer's disease. *Brain*. 2021;144:3505-3516.
39. Sperling RA, Rentz DM, Johnson KA, *et al*. The A4 study: Stopping AD before symptoms begin? *Sci Transl Med*. 2014;6: 228fs213.
40. Rafii M, Sperling R, Donahue MC, *et al*. The AHEAD 3-45 study: design of a prevention trial for Alzheimer's disease. *Alzheimers Dement*. Published online 15 August 2022. doi:10.1002/alz.12748
41. Mintun MA, Lo AC, Duggan Evans C, *et al*. Donanemab in early Alzheimer's disease. *N Engl J Med*. 2021;384:1691-1704.
42. Jack CR Jr, Therneau TM, Lundt ES, *et al*. Long-term associations between amyloid positron emission tomography, sex, apolipoprotein E and incident dementia and mortality among individuals without dementia: Hazard ratios and absolute risk. *Brain Commun*. 2022;4:fcac017.
43. Sperling RA, Mormino EC, Schultz AP, *et al*. The impact of amyloid-beta and tau on prospective cognitive decline in older individuals. *Ann Neurol*. 2019;85:181-193.
44. Knopman DS, Lundt ES, Therneau TM, *et al*. Association of initial beta-amyloid levels with subsequent flortaucipir positron emission tomography changes in persons without cognitive impairment. *JAMA Neurol*. 2021;78:217–228.
45. Sanchez JS, Becker JA, Jacobs HIL, *et al*. The cortical origin and initial spread of medial temporal tauopathy in Alzheimer's disease assessed with positron emission tomography. *Sci Transl Med*. 2021;13:eabc0655.
46. Grothe MJ, Barthel H, Sepulcre J, *et al*. *In vivo* staging of regional amyloid deposition. *Neurology*. 2017;89:2031-2038.
47. Mattsson N, Palmqvist S, Stomrud E, Vogel J, Hansson O. Staging beta-amyloid pathology with amyloid positron emission tomography. *JAMA Neurol*. 2019;76:1319-1329.
48. Collij LE, Heeman F, Salvado G, *et al*. Multitracer model for staging cortical amyloid deposition using PET imaging. *Neurology*. 2020;95:e1538-e1553.
49. Hanseeuw BJ, Betensky RA, Mormino EC, *et al*. PET staging of amyloidosis using striatum. *Alzheimers Dement*. 2018;14: 1281-1292.
50. Michalowska MM, Herholz K, Hinz R, *et al*. Evaluation of *in vivo* staging of amyloid deposition in cognitively unimpaired elderly aged 78–94. *Mol Psychiatry*. 2022;27:4335-4342.
51. Johnson KA, Shultz A, Betensky RA, *et al*. Tau positron emission tomographic imaging in aging and early Alzheimer's disease. *Ann Neurol*. 2016;79:110-119.
52. Therriault J, Pascoal T, Lussier F, *et al*. Biomarker modeling of Alzheimer's disease using PET-based Braak staging. *Nature aging*. 2022;2:526-535.
53. Cho H, Choi JY, Hwang MS, *et al*. *In vivo* cortical spreading pattern of tau and amyloid in the Alzheimer disease spectrum. *Ann Neurol*. 2016;80:247-258.
54. Scholl M, Lockhart SN, Schonhaut DR, *et al*. PET Imaging of tau deposition in the aging human brain. *Neuron*. 2016;89:971-982.
55. Schwarz AJ, Shcherbinin S, Slieker LJ, *et al*. Topographic staging of tau positron emission tomography images. *Alzheimers Dement (Amst)*. 2018;10:221-231.
56. Marquie M, Siao Tick Chong M, Anton-Fernandez A, *et al*. [F-18]-AV-1451 binding correlates with postmortem neurofibrillary tangle Braak staging. *Acta Neuropathol*. 2017;134:619-628.
57. Rullmann M, Brendel M, Schroeter ML, *et al*. Multicenter (18) F-PI-2620 PET for *in vivo* Braak staging of tau pathology in Alzheimer's disease. *Biomolecules*. 2022;12:458.
58. Maass A, Landau S, Baker SL, *et al*. Comparison of multiple tau-PET measures as biomarkers in aging and Alzheimer's disease. *Neuroimage*. 2017;157:448-463.
59. Chen SD, Lu JY, Li HQ, *et al*. Staging tau pathology with tau PET in Alzheimer's disease: A longitudinal study. *Transl Psychiatry*. 2021;11:483.
60. Berron D, Vogel JW, Insel PS, *et al*. Early stages of tau pathology and its associations with functional connectivity, atrophy and memory. *Brain*. 2021;144:2771-2783.
61. Jack CR, Wiste HJ, Weigand SD, *et al*. Defining imaging biomarker cut points for brain aging and Alzheimer's disease. *Alzheimers Dement*. 2017;13:205-216.
62. Wang L, Benzinger TL, Su Y, *et al*. Evaluation of tau imaging in staging Alzheimer disease and revealing interactions between beta-amyloid and tauopathy. *JAMA Neurol*. 2016;73: 1070-1077.
63. Villemagne VL, Dore V, Bourgeat P, *et al*. The tau MeTeR scale for the generation of continuous and categorical measures of tau deposits in the brain: Results from 18F-AV1451 and 18F-THK5351 tau imaging studies. *Alzheimers Dement*. 2016;12: 244.
64. Roberts RO, Geda YE, Knopman DS, *et al*. The Mayo Clinic Study of Aging: Design and sampling, participation, baseline measures and sample characteristics. *Neuroepidemiology*. 2008;30: 58-69.
65. Petersen RC. Mild cognitive impairment as a diagnostic entity. *J Intern Med*. 2004;256:183-194.
66. American Psychiatric Association. *Diagnostic and statistical manual of mental disorders, DSM-IV*. 4th edn. Washington, D.C.: American Psychiatric Association; 1994.
67. Jack CR Jr, Bennett DA, Blennow K, *et al*. NIA-AA research framework: Toward a biological definition of Alzheimer's disease. *Alzheimers Dement*. 2018;14:535-562.
68. Graff-Radford J, Yong KXX, Apostolova LG, *et al*. New insights into atypical Alzheimer's disease in the era of biomarkers. *Lancet Neurol*. 2021;20:222-234.
69. Klunk WE, Engler H, Nordberg A, *et al*. Imaging brain amyloid in Alzheimer's disease with Pittsburgh compound-B. *Ann Neurol*. 2004;55:306-319.
70. Xia CF, Arteaga J, Chen G, *et al*. [(18)F]T807, a novel tau positron emission tomography imaging agent for Alzheimer's disease. *Alzheimers Dement*. 2013;9:666-676.
71. Schwarz CG, Gunter JL, Lowe VJ, *et al*. A comparison of partial volume correction techniques for measuring change in serial amyloid PET SUVR. *J Alzheimers Dis*. 2019;67:181-195.
72. Klunk WE, Koeppe RA, Price JC, *et al*. The centiloid project: Standardizing quantitative amyloid plaque estimation by PET. *Alzheimers Dement*. 2015;11:1-15.
73. Braak H, Braak E. Neuropathological stageing of Alzheimer-related changes. *Acta Neuropathol*. 1991;82: 239-259.
74. Lowe VJ, Lundt ES, Albertson SM, *et al*. Tau-positron emission tomography correlates with neuropathology findings. *Alzheimers Dement*. 2020;16:561-571.
75. Hosmer DW Jr, Lemeshow S, Sturdivant RX. *Applied logistic regression*, vol 398. John Wiley & Sons; 2013.
76. Lowe VJ, Lundt ES, Albertson SM, *et al*. Neuroimaging correlates with neuropathologic schemes in neurodegenerative disease. *Alzheimers Dement*. 2019;15:927-939.
77. La Joie R, Ayakta N, Seeley WW, *et al*. Multisite study of the relationships between antemortem [(11)C]PIB-PET centiloid values and postmortem measures of Alzheimer's disease neuropathology. *Alzheimers Dement*. 2019;15:205-216.
78. Jack CR Jr, Wiste HJ, Lesnick TG, *et al*. Brain beta-amyloid load approaches a plateau. *Neurology*. 2013;80:890-896.

79. Ossenkoppele R, Schonhaut DR, Scholl M, *et al*. Tau PET patterns mirror clinical and neuroanatomical variability in Alzheimer's disease. *Brain*. 2016;139:1551-1567.
80. Ossenkoppele R, Smith R, Ohlsson T, *et al*. Associations between tau, Abeta, and cortical thickness with cognition in Alzheimer disease. *Neurology*. 2019;92:e601-e612.
81. Jack CR, Wiste HJ, Botha H, *et al*. The bivariate distribution of amyloid-beta and tau: Relationship with established neurocognitive clinical syndromes. *Brain*. 2019;142:3230-3242.
82. Hyman BT, Phelps CH, Beach TG, *et al*. National Institute on Aging–Alzheimer's Association guidelines for the neuropathologic assessment of Alzheimer's disease. *Alzheimers Dement*. 2012;8:1-13.
83. Lowe VJ, Wiste HJ, Senjem ML, *et al*. Widespread brain tau and its association with ageing, Braak stage and Alzheimer's dementia. *Brain*. 2018;141:271-287.
84. Vogel JW, Young AL, Oxtoby NP, *et al*. Four distinct trajectories of tau deposition identified in Alzheimer's disease. *Nat Med*. 2021;27:871–881.
85. Young CB, Winer JR, Younes K, *et al*. Divergent cortical tau positron emission tomography patterns among patients with preclinical Alzheimer disease. *JAMA Neurol*. 2022;79: 592-603.
86. Jack CR, Wiste HJ, Weigand SD, *et al*. Predicting future rates of tau accumulation on PET. *Brain*. 2020;143:3136-3150.
87. Sintini I, Martin PR, Graff-Radford J, *et al*. Longitudinal tau-PET uptake and atrophy in atypical Alzheimer's disease. *Neuroimage Clin*. 2019;23:101823.
88. Harrison TM, La Joie R, Maass A, *et al*. Longitudinal tau accumulation and atrophy in aging and Alzheimer disease. *Ann Neurol*. 2019;85:229-240.
89. Vergallo A, Megret L, Lista S, *et al*. Plasma amyloid beta 40/42 ratio predicts cerebral amyloidosis in cognitively normal individuals at risk for Alzheimer's disease. *Alzheimers Dement*. 2019;15:764-775.
90. Mielke MM, Frank RD, Dage JL, *et al*. Comparison of plasma phosphorylated tau species with amyloid and tau positron emission tomography, neurodegeneration, vascular pathology, and cognitive outcomes. *JAMA Neurol*. 2021;78: 1108-1117.
91. Zicha S, Bateman RJ, Shaw LM, *et al*. Comparative analytical performance of multiple plasma Abeta42 and Abeta40 assays and their ability to predict positron emission tomography amyloid positivity. *Alzheimers Dement*. 2022. Published online 12 July 2022. doi:10.1002/alz.12697
92. Shen XN, Huang YY, Chen SD, *et al*. Plasma phosphorylated-tau181 as a predictive biomarker for Alzheimer's amyloid, tau and FDG PET status. *Transl Psychiatry*. 2021;11:585.
93. Meyer PF, Ashton NJ, Karikari TK, *et al*. Plasma p-tau231, p-tau181, PET biomarkers, and cognitive change in older adults. *Ann Neurol*. 2022;91:548-560.
94. Palmqvist S, Stomrud E, Cullen N, *et al*. An accurate fully automated panel of plasma biomarkers for Alzheimer's disease. *Alzheimers Dement*. Published online 11 August 2022. doi: 10. 1002/alz.12751
95. McGrath ER, Beiser AS, O'Donnell A, *et al*. Blood phosphorylated Tau 181 as a biomarker for amyloid burden on brain PET in cognitively healthy adults. *J Alzheimers Dis*. 2022;87:1517-1526.
96. Jagust WJ, Landau SM. Alzheimer's disease neuroimaging I. Temporal dynamics of beta-amyloid accumulation in aging and Alzheimer's disease. *Neurology*. 2021;96:e1347-e1357.
97. Janelidze S, Palmqvist S, Leuzy A, *et al*. Detecting amyloid positivity in early Alzheimer's disease using combinations of plasma Abeta42/Abeta40 and p-tau. *Alzheimers Dement*. 2022;18:283-293.
98. Tissot C, Therriault J, Kunach P, *et al*. Comparing tau status determined via plasma pTau181, pTau231 and [(18)F]MK6240 tau-PET. *EBioMedicine*. 2022;76:103837.
99. Fleisher AS, Pontecorvo MJ, Devous MD Sr, *et al*. Positron emission tomography imaging with [18F]flortaucipir and postmortem assessment of Alzheimer disease neuropathologic changes. *JAMA Neurol*. 2020;77:829-839.
100. Clark CM, Pontecorvo MJ, Beach TG, *et al*. Cerebral PET with florbetapir compared with neuropathology at autopsy for detection of neuritic amyloid-beta plaques: A prospective cohort study. *Lancet Neurol*. 2012;11:669-678.
101. Murray ME, Lowe VJ, Graff-Radford NR, *et al*. Clinicopathologic and 11C-Pittsburgh compound B implications of Thal amyloid phase across the Alzheimer's disease spectrum. *Brain*. 2015; 138(Pt 5):1370-1381.
102. Thal DR, Beach TG, Zanette M, *et al*. [(18)F]flutemetamol amyloid positron emission tomography in preclinical and symptomatic Alzheimer's disease: Specific detection of advanced phases of amyloid-beta pathology. *Alzheimers Dement*. 2015; 11:975-985.
103. Seo SW, Ayakta N, Grinberg LT, *et al*. Regional correlations between [11C]PIB PET and post-mortem burden of amyloid-beta pathology in a diverse neuropathological cohort. *Neuroimage Clin*. 2017;13:130-137.
104. Soleimani-Meigooni DN, Iaccarino L, La Joie R, *et al*. 18F-flortaucipir PET to autopsy comparisons in Alzheimer's disease and other neurodegenerative diseases. *Brain*. 2020; 143:3477-3494.
105. Smith R, Wibom M, Pawlik D, Englund E, Hansson O. Correlation of *in vivo* [18F]flortaucipir with postmortem Alzheimer disease tau pathology. *JAMA Neurol*. 2019;76: 310-317.
106. Janelidze S, Bali D, Ashton NJ, *et al*. Head-to-head comparison of 10 plasma phospho-tau assays in prodromal Alzheimer's disease. *Brain*. Published online 10 September 2022. doi:10. 1093/brain/awac333
107. Hansson O, Edelmayer RM, Boxer AL, *et al*. The Alzheimer's association appropriate use recommendations for blood biomarkers in Alzheimer's disease. *Alzheimers Dement*. 2022;18: 2669-2686.
108. Benedet AL, Brum WS, Hansson O, *et al*. The accuracy and robustness of plasma biomarker models for amyloid PET positivity. *Alzheimers Res Ther*. 2022;14:26.
109. Pascoal TA, Therriault J, Benedet AL, *et al*. 18F-MK-6240 PET for early and late detection of neurofibrillary tangles. *Brain*. 2020; 143:2818–2830.